Peer-reviewed version available at *Water* **2017**, *9*, 540; doi:10.3390/w9070540

Article

Characterisation of Hydrological Response to Rainfall at Multi Spatio-Temporal Scales in Savannas of Semi-Arid Australia

Ben Jarihani [1,*], Roy C. Sidle [1], Rebecca Bartley [2], Christian H. Roth [2] and Scott Wilkinson [3]

[1] Sustainability Research Centre, University of the Sunshine Coast, Australia; bjarihan@usc.edu.au, rsidle@usc.edu.au
[2] CSIRO Land and Water, Brisbane, Australia; Rebecca.Bartley@csiro.au, Christian.Roth@csiro.au
[3] CSIRO Land and Water, Canberra, Australia; Scott.Wilkinson@csiro.au

* Correspondence: bjarihan@usc.edu.au; Tel.: +61-434-194-659

Abstract: Rainfall is the main driver of hydrological processes in dryland environments and characterising the rainfall variability and processes of runoff generation are critical for understanding ecosystem function of catchments. Using remote sensing and in situ data sets, we assess the spatial and temporal variability of the rainfall, rainfall-runoff response, and effects of antecedent soil moisture and ground cover at different spatial scales on runoff coefficients in the Upper Burdekin catchment, northeast Australia, which is a major contributor of sediment and nutrients to the Great Barrier Reef. The high temporal and spatial variability of rainfall exerts significant controls on runoff generation processes. Rainfall amount and intensity are the primary runoff controls, and runoff coefficients for wet antecedent conditions were higher than for dry conditions. The majority of runoff occurred via surface runoff generation mechanisms, with subsurface runoff likely contributing little runoff due to the intense nature of rainfall events. At annual to seasonal temporal scales and for relatively large catchments, we could not detect a significant effect of ground cover on runoff. We conclude that in the range of moderate to large catchments (193 – 36,260 km^2) runoff generation processes are sensitive to both antecedent soil moisture and ground cover. A higher runoff-ground cover correlation in drier months with sparse ground cover highlighted the critical role of cover at the onset of the wet season and how runoff generation is more sensitive to cover in drier months than in wetter months. The monthly water balance analysis indicates that runoff generation in wetter months (January and February) is partially influenced by saturation overland flow, most likely confined to saturated soils in riparian corridors, swales, and areas of shallow soil. By March and continuing through October, the soil 'bucket' progressively empties by evapotranspiration, and Hortonian overland flow becomes the dominant, if not exclusive, flow generation process. The results of this study can be used to better understand the rainfall-runoff relationships in dryland environments and subsequent exposure of coral reef ecosystems in Australia and elsewhere to terrestrial runoff.

Keywords: rainfall-runoff; rainfall variability; Hortonian overland flow; saturation overland flow; ground cover; Burdekin catchment

1. Introduction

The world's coral reefs have undoubtedly been subjected to natural and anthropogenic disturbances and are being degraded [1-6]. It is now well established that the ecological health of the coral reefs is under stress from threats associated with climate change and terrestrial runoff [2-5,7-9]. Runoff from the land, and the sediment and nutrients it carries, are considered to be major factors causing deterioration in the health of the Great Barrier Reef (GBR) [1,3,10] and other coral reefs worldwide [2,4,5,11]. The GBR, a UNESCO world heritage site in north-eastern Australia, is estimated to be worth ~$5.1 billion annually to the Australian economy, exceeding that of agricultural industries adjacent to the GBR [12]. A study of coral reefs between 2007 and 2013 concluded that live coral cover declined by 50% following several weeks of exposure to turbid water from major sediment plumes [13]. Livestock grazing is the dominant land use (~80%) in the catchments draining to the GBR. Terrestrial runoff, fluvial sediment and nutrient discharges are estimated to contribute the majority of the pollutants to the GBR lagoon in Australia and worldwide [2,11,14-16]. Therefore, in-depth investigations of the hydrological processes within these catchments are essential to understand the relationship among rainfall, land management and terrestrial runoff, and the subsequent impacts on pollutant generation and the ecological health of the coral reefs.

There have been a number of studies investigating different aspects of terrestrial runoff to the GBR. At the smaller scale (i.e., plot), studies have established that annual runoff varies considerably with the spatial distribution of ground cover [17], however, cover may have little effect on overland flow during very large rainfall events (>100 mm with intensities between 45-60 mm/hr) when the landscape is inundated with surface runoff due to Hortonian overland flow processes [18-20]. Roth [21] showed that high ground cover values (>75%) can promote infiltration during high intensity events. Even with high cover, localised infiltration varied widely, mainly as a function of macroscopically visible bioturbation by soil macrofauna, such as ants, termites and earthworms. Ground cover is also very 'patchy' in these savanna landscapes [22], which results in variable runoff coefficients even for hillslopes with the same overall cover conditions [17].

At the larger (> 100 km^2) catchment scale, Post [23] regionalised rainfall-runoff (RR) model parameters to predict daily streamflow in ungauged catchments in the Burdekin River basin. A daily lumped parameter RR model (IHACRES) used regionalised model parameters based on catchment physiographic attributes for three portions of the basin: Upper Burdekin, Bowen, and Suttor/lower Burdekin [23]. Although average wet season and daily rainfall data over 24 catchments (68-130,146 km^2) were used, no spatial distribution of rainfall or ground cover was considered. Lough [24] used luminescent lines in corals to reconstruct the history (1685-1981) of major freshwater flows reaching the GBR from the Burdekin River. This study noted that, although there were no overall trends towards wetter or drier conditions since the 17th century, the variability of rainfall and runoff increased during the 20th century with more very wet and very dry extremes than previous periods [24]. Interestingly, trend analysis of stream flow records in northern Australia (Upper Burdekin catchment and Comet catchment) revealed only small impacts of woodland clearing (pre-clearing - 1920-1953, compared to post-clearing - 1979-2007) on both mean and inter-annual streamflow. In the Upper Burdekin some of this increased variability may be the result of baseflow dynamics following tree clearing and increased storm flow during large events [25]. In particular, a series of La Nina events led to an unusual increase in runoff coefficients after clearing. Also, during drought years (2002-2003) with no runoff, annual rainfall in Australian savannas is matched by annual evapotranspiration, and trees extract water from deeper in the soil to maintain transpiration that exceeds rainfall [26]. The influence of ground cover on runoff and soil movement in small plots highlights the relationship between sparse (<40%) ground cover and runoff generation [19]. However, for very large events with high rainfall intensities (> 100 mm/h), cover had little influence on runoff [18,19]. Several studies in the GBR have shown that converting forest to pasture can increase runoff by ~80% at sub-catchment scales [27] and ~40% for river basin scales [28]. Importantly, all of these studies assessed only tree cover, and did not evaluate ground cover (pasture) amount and

condition. Few studies 'assessed' the link between pasture cover and runoff at property or sub-catchment scales because monitoring land management changes over long time scales (> 10 years) is laborious and expensive; however, such long-term measurements are necessary to assess the large natural climate variability in semi-arid rangeland systems [29].

Hydrological processes in the dry tropics differ from other regions as they have greater energy inputs and faster rates of change [30]. Because precipitation is the dominant meteorological driver of runoff generation and soil erosion (including channel and gully erosion processes), analysis of rainfall-runoff data is a basic and essential step to improve our understanding of catchment hydrology [31]. There is also a need to distinguish between the impacts of human activities and climate variability on runoff and sediment generation. Understanding the spatial and temporal variability of the hydroclimate driver (precipitation) is the first step to quantify the effects of changing pasture conditions on the quality and quantity of runoff at both small (plot) and large (catchment) scales.

As evidence of anthropogenic impacts on runoff, trends in ground cover changes were compared with trends in rainfall-runoff records. We assessed hydrological processes using multiple temporal scales from annual to event-based rainfall at nested spatial scales. By assessing multiple scales, we can ascertain whether there is a scale at which differences in land use impacts are detectable, particularly when this signal is measurable and when it is obscured by noise. This assessment allows us to better articulate the appropriate modelling approach and scale to detect impacts of land management on runoff generation processes and subsequently on health of the reef. Finally, we assess rainfall intensity patterns related to erosion potential in different portions of the larger catchment to identify erosion hot spots for evaluating land management practices. Studying relationships among rainfall, land management, and terrestrial runoff are essential for decision makers to better understand and manage these catchments to improve the ecological health of the coral reefs. This research has three main objectives: (1) assess how rainfall and runoff vary over different spatial and temporal scales; (2) assess the effects of ground cover and antecedent soil moisture on catchment hydrologic response; and (3) assess how rainfall regimes affect changes in soil moisture contents and consequently partitioning of overland flow into Hortonian overland flow [HOF; 32] and saturation overland flow [SOF; 33]. These objectives provide the structural sub-headings used the following Methods and Results and Discussions sections.

2. Study site and Materials

2.1. Study site

Here we present the first assessment of long-term spatio-temporal variability of rainfall-runoff data within the Upper Burdekin - a large, dry savannah catchment in northeast Australia. We chose the Upper Burdekin catchment because it has some of the highest runoff and sediment yields of any basin draining to the GBR [34,35]. The Upper Burdekin catchment drains above Sellheim Gauging station covering 36,260 km^2 (Figure 1). Elevation ranges from 217 to 1036 m a.s.l. (mean = 511) and average slope of the catchment is 4.85%. The catchment is largely undeveloped and is characterised by extensive eucalypt savanna woodlands [21]. Livestock grazing occupies most of the catchment (88.3%), with defence (5.5%), managed resource protection areas (3.1%), national parks (2.4%), and marsh/wetlands (0.7%) occupying the remaining areas. Vegetation cover derived from Landsat images from 2000 to 2010 show that 21.2% of the Upper Burdekin is covered by woody vegetation [36]. Soils are mostly shallow (mean depth = 0.25 m) with average depth to bedrock of 0.85 m [37]. Soils are generally weathered, sodic, and mostly red duplex soils that overlie shallow bedrock [38]. Large areas of yellow and brown spodisols are found near streams and gullies [39]. Basaltic sub-catchments in the central-west portion of the catchment have vertisol or ferrosol soils with high levels

of phosphorus sourced from basalts [40]. Generally soils have low to moderate fertility and, due to their clay surface texture and grazing pressure, surfaces are prone to crusting and hard-setting [38].

Nine telemetered stream gauging stations are nested within the Upper Burdekin operated by the Queensland Government with contributing areas ranging from 193 to 36,260 km^2 and historical records ranging from 3.6 to 51.4 years (Table 1). The long term (1889-2016) mean annual precipitation within the catchment is 710 mm/year, which produces mean annual runoff of 131 mm/year (rainfall-runoff ratio of 18%). According to Australian Water Availability Project [AWAP; 41] data, the average annual Priestley-Taylor potential evaporation in the catchment is 1734 mm/year.

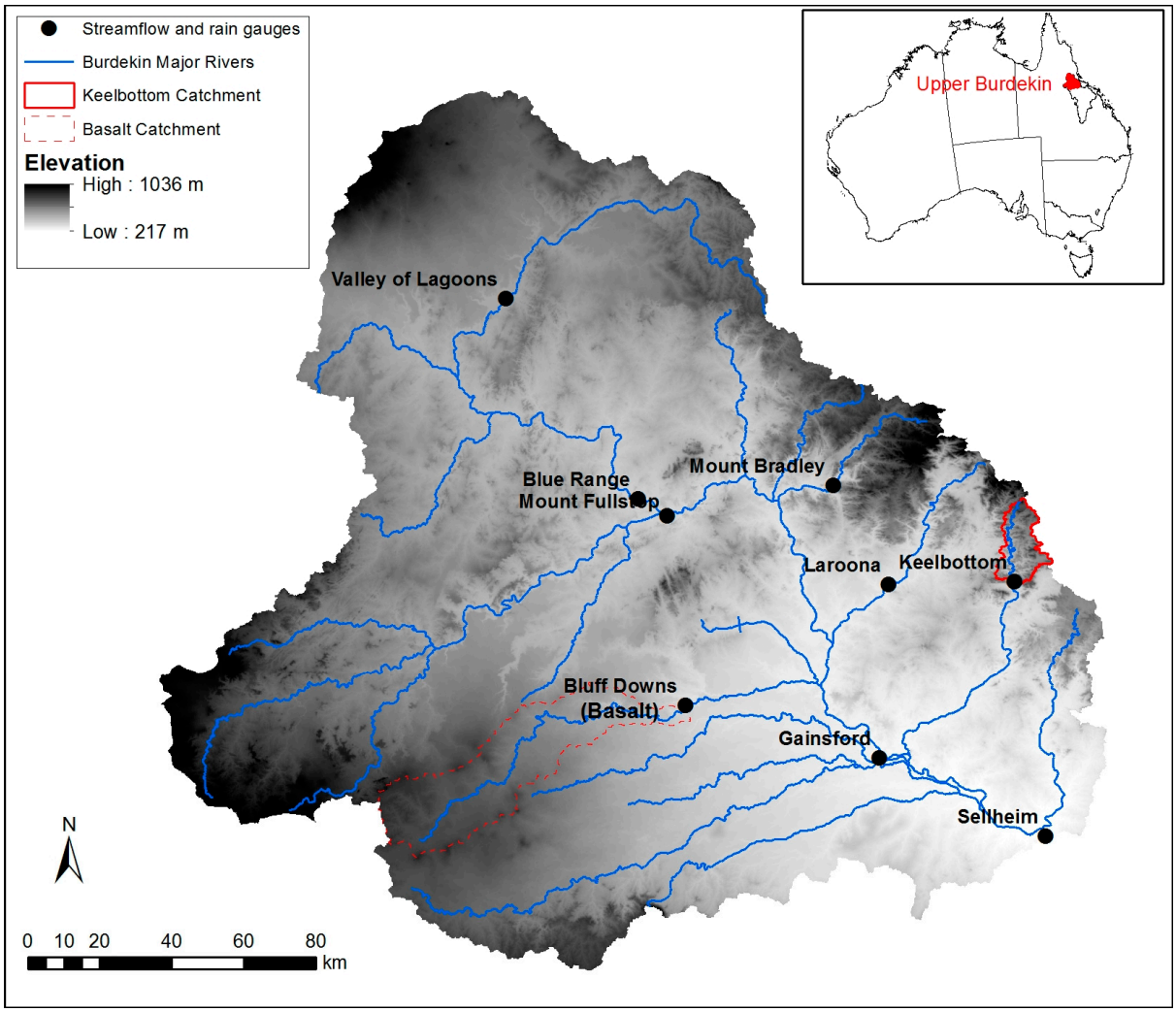

Figure 1. Study site location and rainfall/discharge gauging sites location. Upper Burdekin basin is highlighted in red on the inset map.

Table 1. Characteristics of the currently operational stream gauging stations in the Upper Burdekin Catchment.

Site Name	Site no.	River Name	Latitiude	Longitude	Site commenced	Data period (year)	Catchment area (km^2)	Mean annual rainfall ($mm\ y^{-1}$)	Mean annual PET ($mm\ y^{-1}$)	Mean runoff ratio %
Sellheim	120002C	Burdekin	20.01° S	146.44° E	1/Oct/1968	47.7	36260	707	1748	15
Keelbottom	120102A	Keelbottom	19.37° S	146.36° E	23/Aug/1967	48.8	193	1294	1713	35
Bluff Downs	120106B	Basalt	19.68° S	145.54° E	1/Oct/1967	48.7	1283	664	1730	8
Blue Range	120107B	Burdekin	19.16° S	145.42° E	1/Oct/1982	33.7	10530	698	1738	12
Mount Fullstop	120110A	Burdekin	19.21° S	145.50° E	16/Jan/1965	51.4	17310	688	1740	11
Laroona	120112A	Star	19.38° S	146.05° E	1/Oct/1967	48.7	1212	1172	1757	30
Mount Bradley	120120A	Running	19.13° S	145.91° E	12/Mar/1975	41.3	490	1306	1686	28
Gainsford	120122A	Burdekin	19.81° S	146.02° E	3/Jun/2004	12.0	26320	721	1744	15
Valley of Lagoons	120123A	Burdekin	18.66° S	145.09° E	23/Oct/2012	3.6	3509	766	1754	8

2.2. Materials

2.2.1. Rainfall and streamflow data

We used daily gridded precipitation data from Scientific Information for Land Owners (SILO; https://www.longpaddock.qld.gov.au/silo/index.html) database of the Queensland Government [42,43]. SILO is a historical climate database for Australia constructed from observational records and provides daily weather data from 1889 to present. Gridded datasets are interpolated surfaces which are stored on a regular 0.05 by 0.05 degree (~ 5 by 5 km) grid. There are 38 daily rain gauges in Upper Burdekin catchment that were used to calculate gridded data. In addition to daily rainfall data, there are nine sub-daily recording (tipping bucket) rain gauges in the Upper Burdekin at locations adjoining Queensland Government river/stream gauges (Figure 1). Tipping buckets have variable time steps and whenever the 2 mm bucket is filled, it empties and time is recorded. Therefore the time interval is variable based on rainfall intensity.

River and stream runoff data from nine gauging stations in 15 min, hourly, daily, monthly and annual intervals are available from Department of Natural Resources and Mines (DNRM) Water Monitoring Information Portal (WMIP; https://water-monitoring.information.qld.gov.au/).

2.2.3. Actual evapotranspiration

We used MODIS satellite Global Evapotranspiration (MOD16; http://www.ntsg.umt.edu/project/mod16) datasets that are part of the NASA/EOS project to estimate global terrestrial evapotranspiration from land surfaces. MOD16 products include 8-day, monthly, and annual actual evapotranspiration (AET) and potential ET (PET) datasets in regular 1 km^2 land surface grids from 2000 to 2014. The MOD16 ET datasets are estimated using the Mu, *et al.* [44] ET algorithm that is based on the Penman-Monteith equation. MOD16 AET datasets include evaporation from wet and moist soil, from rain water intercepted by the canopy before it reaches the ground, and the transpiration through vegetation leaves and stems.

2.2.4. Ground cover data

We used seasonal fractional ground cover derived from USGS Landsat images (30 by 30 m resolution) by Remote Sensing Centre of the Department of Science, Information Technology and Innovation (DSITI). These data also are available through the AusCover website (http://www.auscover.org.au/xwiki/bin/view/Product+pages/Seasonal+Ground+Cover) for at least one image per standard calendar season since 1990. We also used MODIS-derived monthly vegetation fractional cover images at coarser (500 by 500 m) spatial resolution. MODIS fractional cover data represent the exposed proportion of Photosynthetic Vegetation (PV), Non-Photosynthetic Vegetation (NPV) and Bare Soil (BS) within each pixel [45]. This dataset is publically available from the Auscover website (http://www.auscover.org.au/).

2.2.5. Soil moisture

The Soil Water Index (SWI) product of Copernicus Global Land service [46] was used to assess moisture conditions driven largely by precipitation and subsequent infiltration at various depths into the soil. The SWI was first proposed by Wagner [47] and is a method for estimating the soil moisture profile from surface observations based on only one parameter (T), which is related to infiltration time [48]. SWI data are derived from the METOP-ASCAT sensor and are available from 2007 to present in 0.1 degree (~ 10 by 10 km) spatial resolution for daily and 10-day temporal frequencies. SWI is available globally via the Copernicus website (http://land.copernicus.eu/global/products/swi).

3. Methods

3.1. Rainfall and runoff spatio-temporal variability

3.1.1. Variation in rainfall amount

We assessed long term spatial and temporal variability of rainfall in the nested catchments above the nine gauging stations (Table 1). First, SILO gridded rainfall data were clipped for each sub-catchment and spatially averaged over the catchment areas to calculate mean daily rainfall. Then monthly and annual rainfall data were calculated from daily data. The annual data analysis is based on a water year (1 July to 30 June of the next year), thus placing the Austral summer monsoonal season near the middle of the water year. Temporal variability of rainfall is calculated by using the standard deviation in each 5 km grid for all annual rainfall records.

To assess the temporal variability in rainfall, following Food and Agricultural Organization's (FAO) protocols [49], we used the following rules to determine dry, normal, and wet weather conditions: (1) condition in a period is called dry if the rainfall received during that period has a probability of exceedance of > 80%; (2) normal if it has a probability of exceedance of 20-80%; and (3) wet if it has a probability of exceedance of < 20% [49]. Daily rainfall data (>2 mm d^{-1}) over seven catchments of Upper Burdekin were used in probability of exceedance calculations.

3.1.2. Variation in rainfall intensity

The degree to which rainfall amount and intensity vary across an area and/or through time is an important characteristic of the climate that influences runoff generation processes [50]. Variability in rainfall intensity throughout the Upper Burdekin catchment was also investigated using sub-daily rainfall records from nine rain gauges. The RIST (Rainfall Intensity Summarisation Tool) is used to analyse intensity by organizing rainfall data into specific time intervals (5, 10, 15, 20, 30 and 60 min, and daily) [51]. The program uses inputs of raw rainfall data to create outputs of rainfall amount, intensity, and kinetic energy per time interval [51]. RIST is also used to conduct storm analyses for events above 2 mm, 5 mm and 10 mm, and identifies characteristics of each event. Kinetic energy calculation is based on rainfall intensity values by using the McGregor, *et al.* [52] equation.

3.1.3. Variation in runoff

Monthly and annual volumetric runoff ratios for each sub-catchment were calculated from accumulated rainfall and runoff for each catchment (runoff/rainfall). The effect of rainfall spatial variability on runoff was assessed by comparing runoff ratios of two sub-catchments with high (Keelbottom; 1294 mm/year on average) and low (Basalt; 664 mm/year on average) rainfall.

3.2. Changes in land surface conditions

Land surface condition affects rainfall-runoff processes and alters the amount of rainfall that can infiltrate and be stored in the soil profile or runs off the catchment. The effects of ground cover and antecedent soil moisture on runoff generation were assessed using the Landsat-derived seasonal Ground Cover (GC) data of Australia to estimate the 'true' ground cover for each season. GC is restricted to areas of less than 60% woody vegetation by combining information from the persistent green products and seasonal fractional cover products [53]. The GC metrics (green, non-green and bare ground) for each water year were calculated by averaging seasonal metrics. We also used MODIS-derived monthly fractional data to compare with seasonal Landsat-derived data to explore the changes in ground cover changes in monthly time periods.

To assess the effect of soil moisture on runoff generation, the SWI daily products were extracted for each catchment and then averaged into monthly and annual data. The effect of ground cover on runoff generation was evaluated by simple linear correlation between monthly ground cover and runoff ratio. To assess the relative influence of soil moisture versus ground cover on runoff, a multiple

regression analysis was used. Rainfall, soil moisture, and ground cover were the independent variables in the regression analysis used to predict runoff (dependent variable) for annual time steps between water years 1990-1991 and 2015-16. Multiple correlation coefficient, coefficient of determination and standard error statistical parameters were calculated and compared for these 26 water years.

To eliminate the effect of rainfall variability, we compared two months (November and April) with similar long term monthly rainfalls, but with different ground cover in Upper Burdekin catchment. The hypothesis was that the slope of the linear correlation between ground cover and runoff ratio should be steeper in November than April. In other words, if ground cover and associated soil condition is important for controlling the proportion of rainfall that turns into runoff (or the runoff ratio) in these catchments, then similar rainfall in November (driest period) should produce more runoff compared to a similar event in April (wet period), as soil saturation is the controlling process. With soils in certain catchment locations being saturated in April (end of the wet season), there is more chance for precipitation becoming runoff than as opposed to November (end of the dry / start of the wet season).

3.3. Changes in soil moisture conditions

A water balance (Eq. 1) was used to assess how the temporal variability of rainfall affects overland flow. To estimate available water in the soil profile (S) for annual and monthly time steps, we performed a simple water balance by subtracting outputs from inputs. With no irrigation, rainfall (P) is the only input to the soil 'bucket' and exfiltration from groundwater or other inputs are negligible [26]. Runoff (R) and actual evapotranspiration (AET) are the water losses from the system. Infiltration into the soil contributes to evaporation from the soil surface, transpiration by vegetation, and percolation and storage into much deeper soil layers. However, discharge into deeper groundwater is negligible for monthly and annual time intervals. Therefore following [54] a simplified mass balance equation (1) is used:

$$P_t - R_t - AET_t = \Delta S, \quad (1)$$

where t is time period (monthly and annual in this study). We calculated the monthly and annual changes in water storage from P, R and AET parameters for all catchments for the time period (2000-2014).

To eliminate the influence of multiple small rain events, which contribute little or no runoff, but may accumulate over long periods, several thresholds were defined. Total event rainfall greater than various threshold values (i.e., 5, 10, 15, 20, 25, 30, 40 and 50 mm) were correlated against runoff in each catchment to improve the runoff ratio calculations.

4. Results and Discussion

4.1. Rainfall and runoff spatio-temporal variability

4.1.1. Variation in rainfall amount

Throughout the Upper Burdekin catchment, long-term (1889-2016) annual rainfall varies between 560 and 2300 mm/year, with a mean rainfall of 710 mm/year and a standard deviation of 176 mm/year (Figure 2). In general, annual rainfall decreases from east to west; however, the variability of rainfall east of the Burdekin River is 10 times higher (~20 mm / linear km) than the west side of the catchment (~2 mm / km). The Upper Burdekin has experienced above average rainfall in 57 years and below average rainfall in 70 years in the last 127 years of record. Probabilities of exceedance of 20% (wet), 50% (normal), and 80% (dry) rainfall in the Upper Burdekin correspond to annual precipitation values of 895, 672, and 492 mm/year, respectively. A comparison of one wet (Keelbottom Creek in the east) and one dry (Basalt River in the west) sub-catchment highlight the diverse rainfall conditions within the

Preprints (www.preprints.org) | NOT PEER-REVIEWED | Posted: 13 June 2017 doi:10.20944/preprints201706.0056.v1

Peer-reviewed version available at Water 2017, 9, 540; doi:10.3390/w9070540

Upper Burdekin. The Basalt sub-catchment is considerably drier (wet: 880 mm/year, normal: 620 mm/year, dry: 445 mm/year) than Keelbottom (wet: 1700 mm/year, normal: 1260 mm/year, dry: 825 mm/year).

It has been demonstrated that rainfall amount and intensity variation influence runoff generation in small-scale experimental plots [19,21]. However, at the catchment scale, heterogeneity in rainfall magnitude and intensity can have a significant impact on the runoff and hydrological processes.

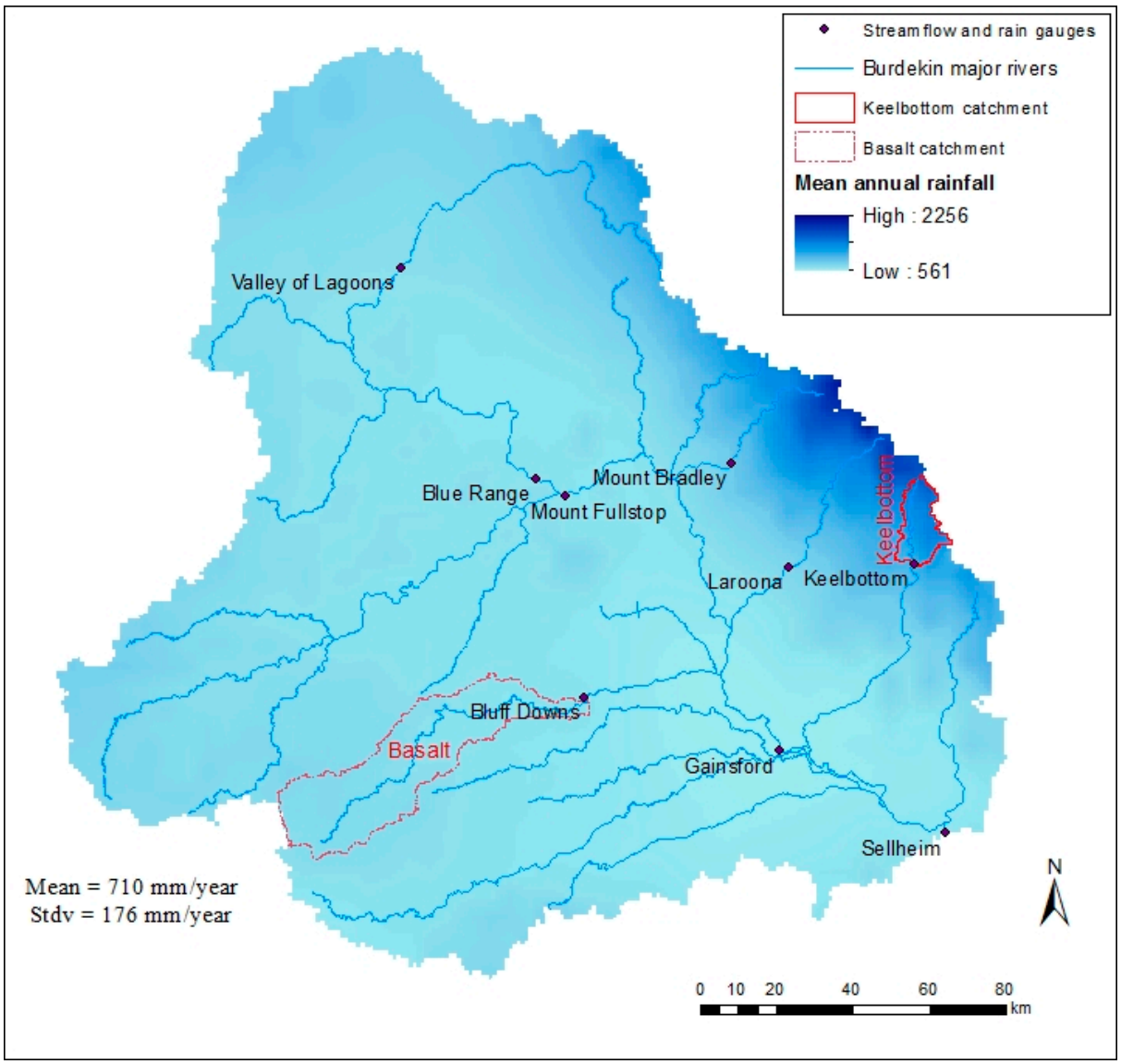

Figure 2. Distribution of long term (1889-2016) annual rainfall of Upper Burdekin catchment. This map is based on daily gridded 5x5 km rainfall data from SILO.

Temporal distribution of rainfall in the Upper Burdekin (Figure 3a) displays the typical summer dominant, monsoonal rainfall pattern of Northern Australia, with December to March being the wetter months. Ignoring the interaction between surface and groundwater and assuming that soil moisture is relatively the same at the beginning of each water year, the actual evapotranspiration of the catchment can be calculated from precipitation (710 mm/year) minus runoff (131 mm/year). Using the Budyko framework [55], low annual rainfall and actual evapotranspiration (579 mm/year) compared with

potential evapotranspiration (~ 1800 mm) indicate that the Upper Burdekin catchment is categorised as a water-limited (dry) environment, although some of the wetter areas on the eastern fringes of the catchment would be classified as energy-limited (i.e., wet) environment. Therefore this system is classified as equitant, where water-limited and energy-limited conditions are experienced on a sub-annual time-step [56]. Monthly actual evapotranspiration and runoff follow similar trends with monthly precipitation maxima in December through March. These four months contribute 74% of the annual precipitation, 89% of annual runoff, and 70% of actual evapotranspiration (Figure 3a). This summer dominant rainfall pattern in the Upper Burdekin exhibits high inter-annual and decadal variability of rainfall, similar to rainfall variability across northern Australia and Queensland [57]. This high variability is closely linked with El Niño–Southern Oscillation (ENSO) events with above average rainfall during La Niña events and drier conditions during El Niño events [24]. Excluding minor events (< 2 mm) from intensity calculations eliminates numerous small rainfalls from the analysis and more realistically reflects the correct number of storms and magnitude-intensity relationships. These larger storms are directly associated with the majority of runoff generation [19] and erosion [17].

Preprints (www.preprints.org) | NOT PEER-REVIEWED | Posted: 13 June 2017 doi:10.20944/preprints201706.0056.v1

Peer-reviewed version available at Water 2017, 9, 540; doi:10.3390/w9070540

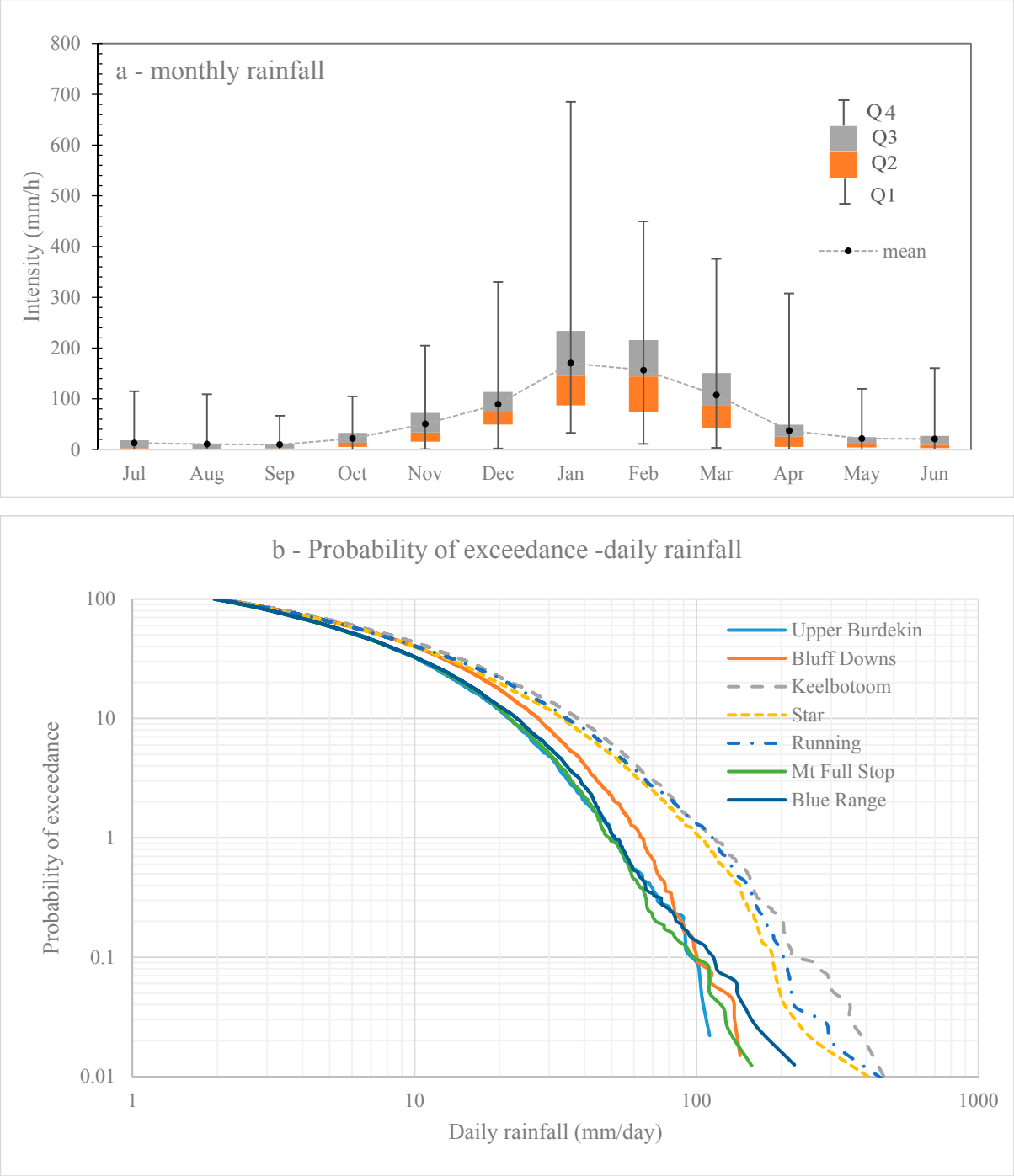

Figure 3. Temporal distribution of the rainfall in Upper Burdekin. (a) – Long term mean monthly rainfall distribution. Boxes show quartiles (denoted Q): Q2 (median or 50%), and Q3 (75%). Average of total rainfall in each month was used to calculate means. Whiskers show the maximum Q1, and minimum Q4, of rainfall records in each month. (b) Probability of exceedance for daily rainfall data (>2 mm) over seven catchments of Upper Burdekin. Gainsford and Valley of Lagoons catchments are excluded due to shorter data records. Wet (eastern) catchments are presented in dashed-line and drier (western) catchments have continuous lines.

Daily rainfall probability of exceedance, PE (probability of the occurrence of a daily rainfall depth >2 mm), was calculated for all catchments (Figure 3b). Two types of rainfall exceedance relationships can be distinguished in Fig 3b. The Keelbottom, Star and Running rivers have a significantly higher

probability of exceedance of rainfall than the drier catchments. The long-term (1889-2016) annual average number of rainy days (total rain > 2 mm) varied over the Upper Burdekin catchment, ranging from 60 to 170 days per year with an average of 100 days per year and a standard deviation of 20 days per year. The spatial distribution of rainy days follows the same pattern as rainfall depth; higher in the east and lower in the west. The temporal variability of rainy days per annum for 1889-2016 varied from 57 to 195 days per year.

4.1.2. Variation in rainfall intensity

From the nine gauges in the Upper Burdekin, only five rain gauges (Keelbottom, Basalt, Blue Range, Mount Fullstop, and Laroona) have long-term (i.e., 1998-2016) sub-daily records. As expected, higher intensities are associated with shorter duration rainfalls. Maximum recorded 15, 30 and 60 min rainfall intensities in the Upper Burdekin are 220, 115, and 93 mm/h, respectively. Interestingly, the rainfall intensities are similar across the catchment for the more frequent lower intensities, but marginally different between east and west for very rare (< 0.01% PE) high intensity events.

Preprints (www.preprints.org) | NOT PEER-REVIEWED | Posted: 13 June 2017 doi:10.20944/preprints201706.0056.v1

Peer-reviewed version available at Water 2017, 9, 540; doi:10.3390/w9070540

Intensities were assessed on an annual and monthly scale to quantify the temporal variability of intensities at each of the five rain gauges (Figure 4). Fixed time intervals (5, 10, 15, 30, 60 min and daily) for the continuous precipitation records and individual storm method were used in the intensity analysis. Because these methods yielded similar results, we present 30 min fixed time interval results in Figure 4. In both methods, events with < 2 mm of rain were excluded from intensity analysis. Results revealed that although the magnitude of rainfall intensities are similar at all five gauge stations (Figure 4a), the number of storms and consequently the total kinetic energy is higher in wetter sub-catchments (i.e., Keelbottom) than drier catchments (i.e., Basalt). Water years 1999-2000, 2008-2009 and 2010-2011 had the highest number of rainfall records and higher total kinetic energy (Figure 4c). The median rainfall intensities for all periods (5, 10, 15, 30, 60 min and daily) had their minimum and maximum values during dry water year 2006-2007 and wet year 2010-2011, respectively.

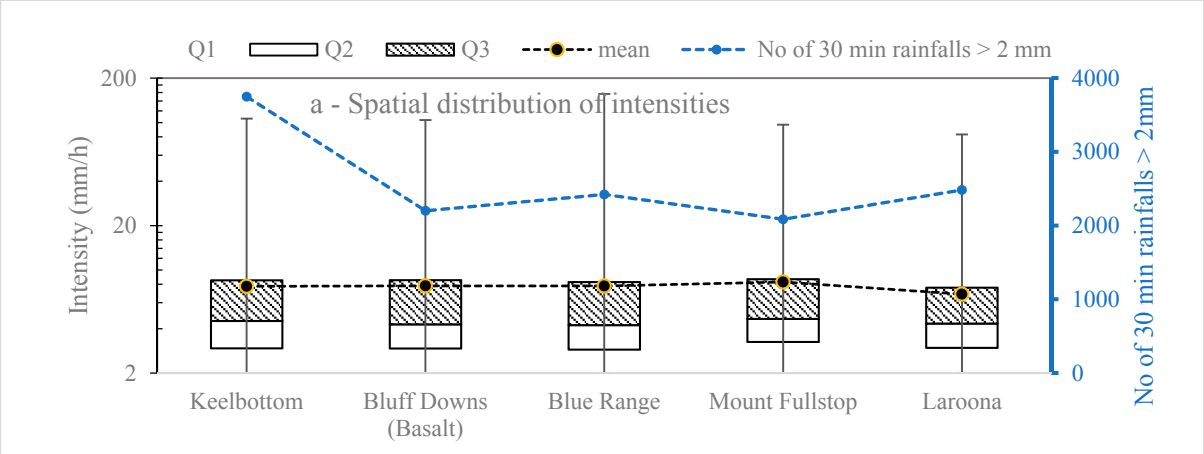

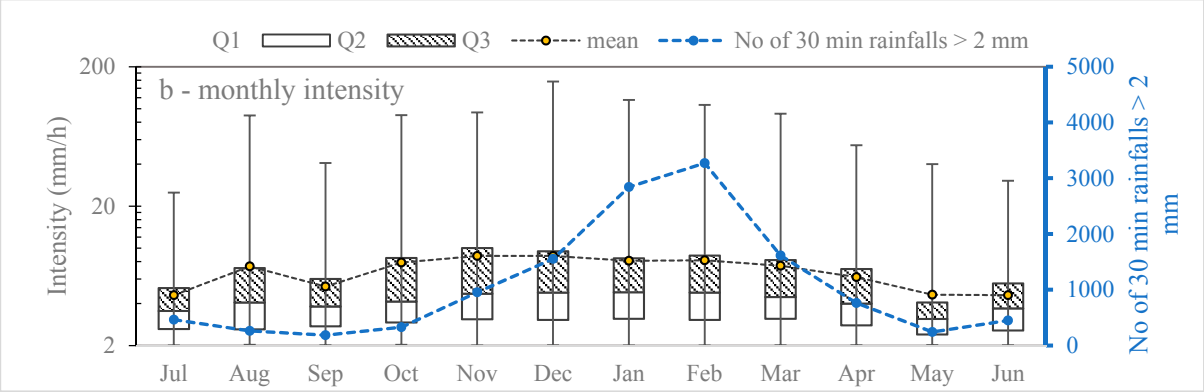

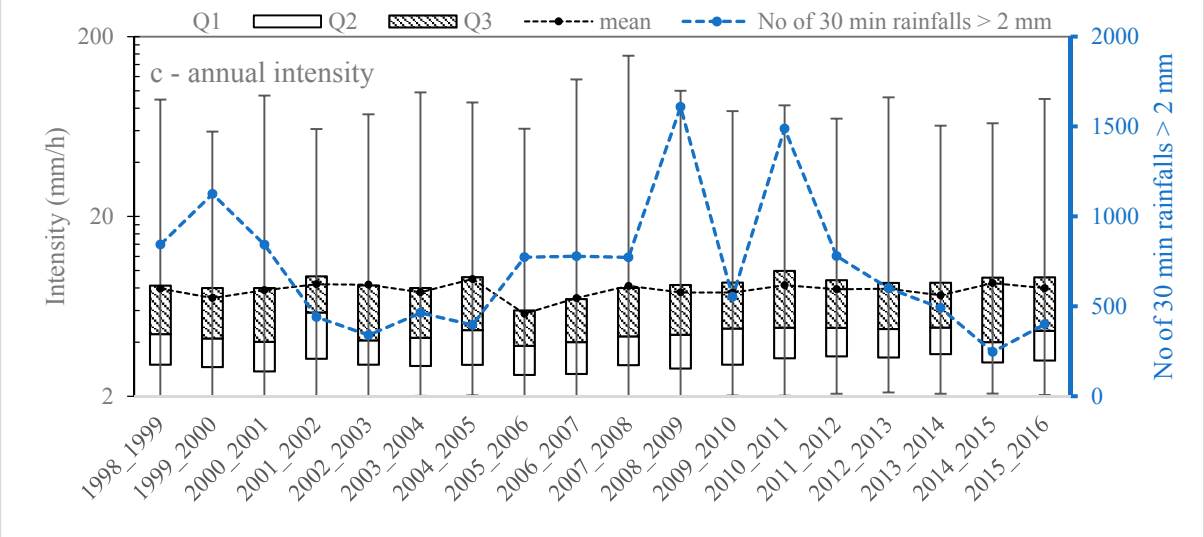

Figure 4. Spatial and temporal rainfall intensity variation in Upper Burdekin from 1998 to 2016. (a): Spatial distribution of the rainfall intensities for fixed interval 30 min rainfalls with > 2 mm of total rain at the location of five rain gauges (Keelbottom, Basalt, Blue Range, Mount Fullstop and Laroona). (b) Monthly intensity (average of five gauging stations) distribution of 30 min fixed interval rainfalls. (c) Annual intensities from 1998-2016 (averages of five gauging stations). In all parts a-c, box plots show quartile 1, quartile 2 (median), quartile 3 and quartile 4 of the intensities, and whiskers represent minimum and maximum values. Mean values and number of events with > 2 mm of total rain are also presented as dashed lines.

Monthly rainfall intensity analysis revealed that rainfall intensities are higher during November to April than the rest of the year (Figure 4b). Although the number of rainfall events and total depths of rainfall are highest in February, the mean and median of the intensities are similar throughout the wet months (December – March) then decrease from April to November. Annual runoff ratios were highly correlated with mean rainfall intensities for all five rain gauges (Keelbottom; $R^2 = 0.67$, Basalt; $R^2 = 0.52$, Blue Range; $R^2 = 0.74$, Mount Fullstop; $R^2 = 0.71$ and Laroona; $R^2 = 0.67$). All five rain gauges are located at the catchment outlet adjacent to water level instruments.

Individual storm analysis revealed that there are a higher number of storms in wetter catchments than in drier catchments. For example, the number of storms in Keelbottom catchment is almost double the number in Basalt catchment and consequently the kinetic energy [52] that causes soil erosion is also higher in Keelbottom.

4.1.3. Runoff variability

Runoff data for the entire Upper Burdekin catchment are available since 1948 at the Sellheim gauging station. Annual runoff varies from 5 to 680 mm/year with an average of 130 mm/year. The annual rainfall-runoff relationship for the Upper Burdekin indicates that the annual rainfall needed to trigger runoff is ~300 mm/year; (Figure 5a). As in other catchments worldwide, soil characteristics (e.g., depth) and geology have significant effects on regional streamflow regime [58,59]. For example, the rainfall-runoff relationships for Basalt and Keelbottom catchments differ substantially. Annual rainfall required to trigger runoff in the Keelbottom catchment, with more rainfall, is higher (~550 mm) than in the Basalt catchment (~200 mm). This difference could be attributed to the greater forest cover in Keelbottom (>70%) compared to Basalt (<10%) that would buffer runoff during drier conditions together with the greater rooting depth of trees that would promote infiltration and soil water storage available for evapotranspiration [59,60]. Differences in soil depth, hydraulic conductivity, and surface geology could also play a role [31]. However, once runoff is generated, the rate of increase in discharge per unit change of rainfall is higher in the wetter (Keelbottom) catchment. The implication is that the more heavily vegetated savanna catchments require more antecedent rainfall to generate runoff than in drier, poorly vegetated catchments.

The temporal volumetric annual runoff ratio (runoff /rainfall) for the Upper Burdekin varies from 0.01 to 0.48 with an average of 0.15. Spatially, this runoff ratio is higher for humid parts of the catchment compared to dry regions. For example, the average annual runoff ratio for Keelbottom (0.01-0.91, mean = 0.35) is five-fold higher than Basalt (0.0-0.32, mean = 0.07).

Preprints (www.preprints.org) | NOT PEER-REVIEWED | Posted: 13 June 2017 doi:10.20944/preprints201706.0056.v1

Peer-reviewed version available at Water 2017, 9, 540; doi:10.3390/w9070540

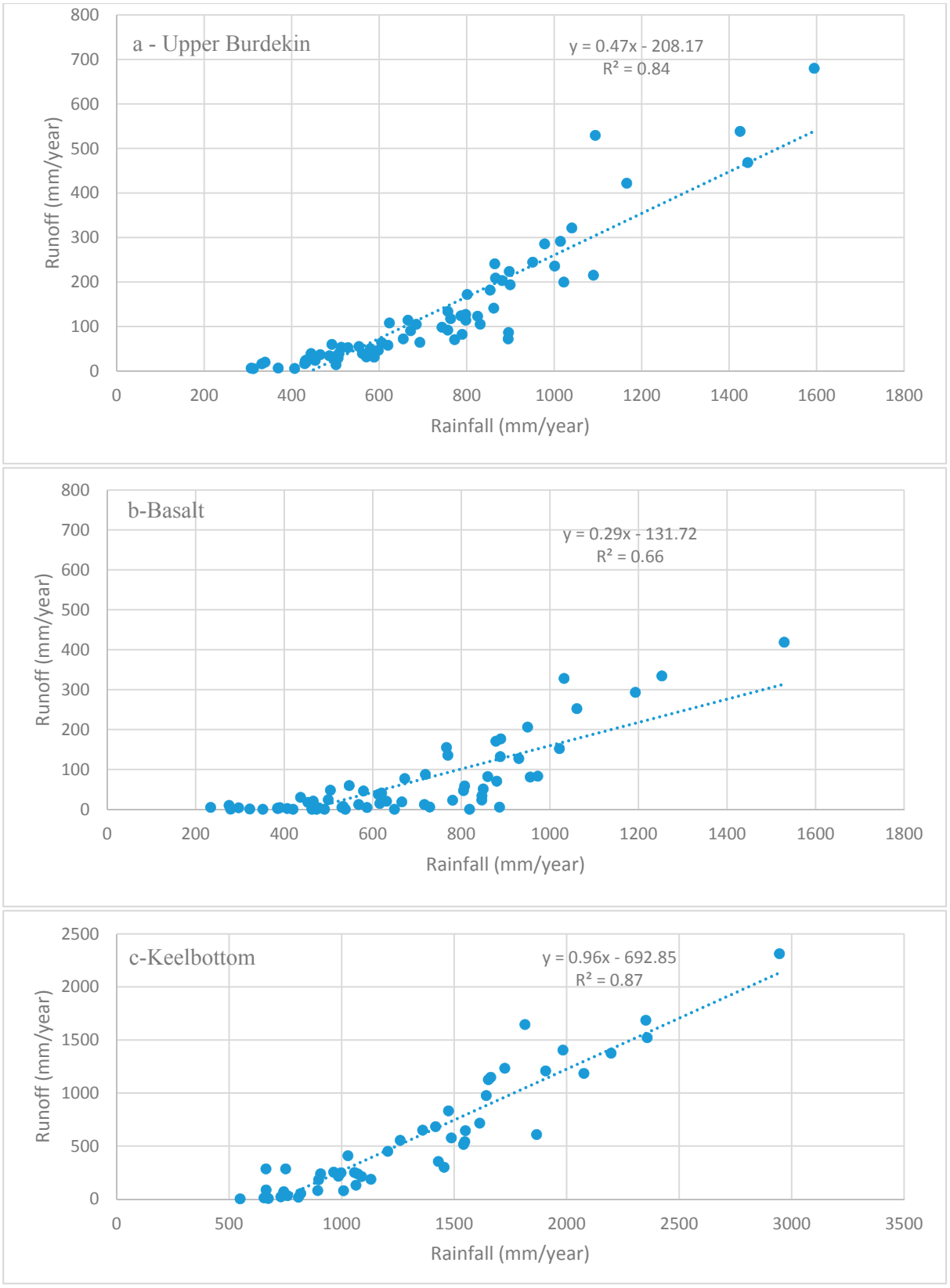

Figure 5. Annual rainfall-runoff relations in Upper Burdekin catchment above Sellheim, Basalt and Keelbottom gauge stations for the period of 1948-2016.

The annual runoff ratio positively correlates with the magnitude of total annual rainfall (P: R^2 = 0.78) and runoff (R: R^2 = 0.92), and was higher (P: R^2 = 0.80, R: R^2 = 0.96) for above average rainfall years (wet years) than below average dry years (P: R^2 = 0.59, R: R^2 = 0.92). Average monthly runoff from the Upper Burdekin in the period from 1948 to 2016 ranged between zero (August-October) and 45 mm (February) (Figure 6). Although January (33 mm) and February (45 mm) have higher rainfall than March (31 mm), the runoff ratio in March (0.27) is higher than January (0.12) and February (0.2) due to higher antecedent soil moisture [61,62]. Runoff ratios are low at the start of the wet season in November and increase from December to March due to increases in soil moisture. Despite low to zero rainfall from April to September, runoff ratios are also high, most likely due to carry-over soil moisture from previous months and/or lag associated with base flow generation.

Preprints (www.preprints.org) | NOT PEER-REVIEWED | Posted: 13 June 2017 doi:10.20944/preprints201706.0056.v1

Peer-reviewed version available at Water 2017, 9, 540; doi:10.3390/w9070540

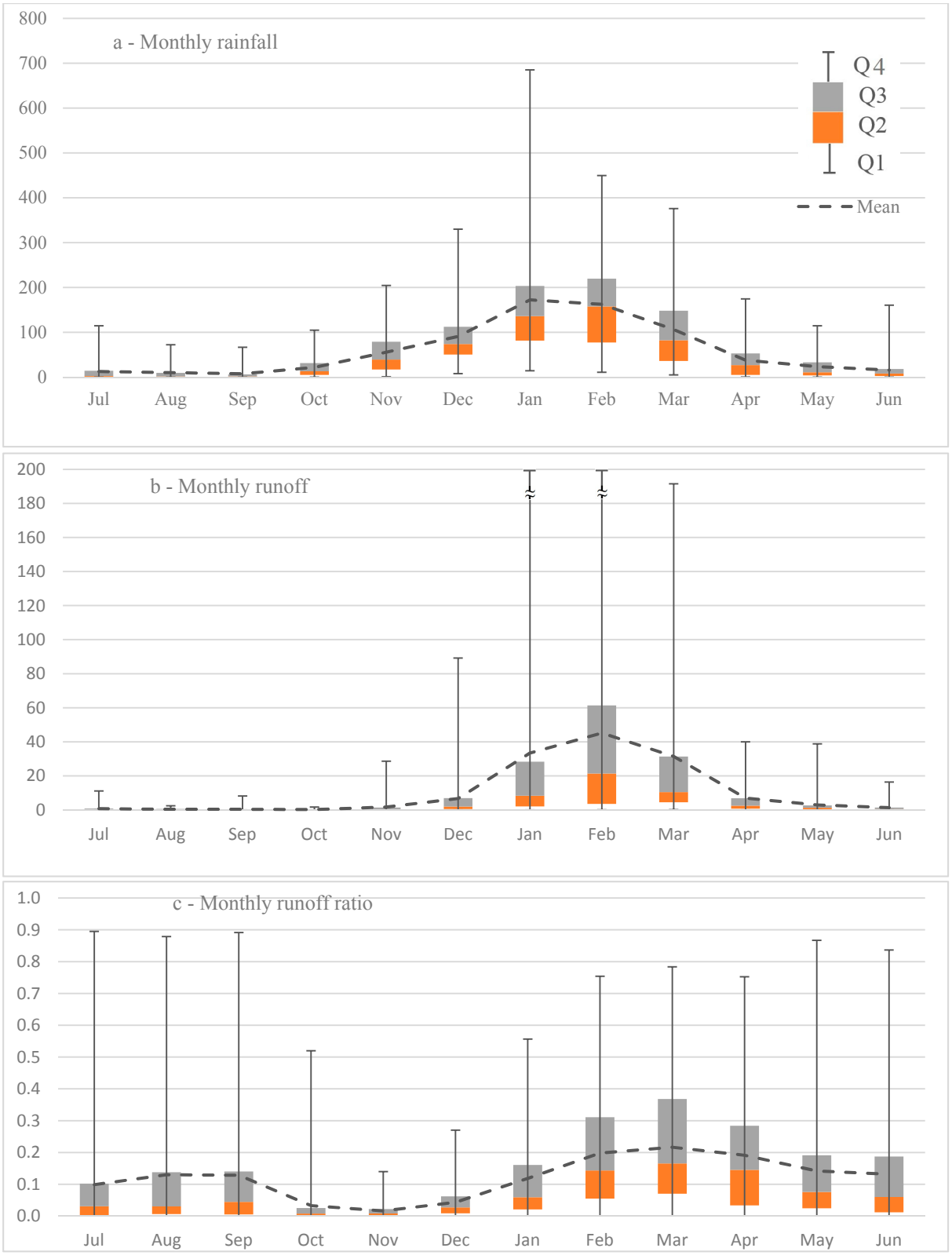

Figure 6. Distribution of monthly rainfall, runoff and runoff ratio in Upper Burdekin. Monthly analysis is based on data records at Sellheim gauging station 1948-2016.

4.2. Changes in land surface conditions

Seasonal ground cover data generated from Landsat, and monthly fractional cover from MODIS were extracted and compared with rainfall data over the Burdekin catchment from 1990 to 2016 (Figure 7). Ground cover data consists of Photosynthetic Vegetation (PV), Non-Photosynthetic Vegetation (NPV) and Bare Soil (BS) within each pixel; the total vegetation (TVC) cover is calculated as PV + NPV. The annual total cover varies from 72% during the 1990-1995 drought to 95% in the wet period of 2010-2011, acknowledging that Landsat-derived ground cover estimates can over-predict cover by up to 20% when compared to on-ground measurements at the hillslope scale [17,63]. Seasonal green cover exhibited weak agreement with rainfall of the previous season (r = 0.5), however, the correlation of seasonal green cover with rainfall in the same season was slightly higher (r = 0.6), suggesting that seasonal periods are too long to investigate vegetation changes due to rainfall variation and also is too long to assess lag times. In contrast, monthly green cover from MODIS was weakly related with rainfall of the same month (r = 0.44), more strongly related with rainfall of the previous month (P_{t-1}; r = 0.69), and had the strongest relationship with total rainfall of the two previous months ($P_{t-2} + P_{t-1}$; r = 0.81) across all catchments. These higher correlations highlight sub-seasonal response time of the dryland savanna systems to individual rainfall events (Figure 7).

Multiple regression analysis of the annual runoff time series of Upper Burdekin catchment showed that using only antecedent soil moisture to predict runoff was the worst option, followed by ground cover alone, and combination of ground cover and soil moisture (Table 2). Using rainfall as the only predictor increased runoff predictions dramatically and additions of GC and SM only further improved R^2 slightly (Table 2). Comparing effects of soil moisture versus ground cover on runoff revealed that for annual time steps, runoff is more sensitive to ground cover than soil moisture.

Table 2. Statistical parameters of multilinear regression analysis of Runoff (R) vs. rainfall (P), ground cover (GC) and Soil moisture (SM). Correlation increases from left to right.

	R vs. SM	R vs. GC	R vs. GC&SM	R vs. P	R vs. P&SM	R vs. P&GC	R vs. P&GC&SM
Multiple R	0.34	0.44	0.45	0.90	0.90	0.91	0.93
R^2	0.12	0.19	0.20	0.81	0.81	0.83	0.86
Adjusted R^2	0.08	0.16	0.13	0.80	0.79	0.81	0.85
Standard Error	148.6	141.87	144.22	68.65	70.08	66.99	60.90

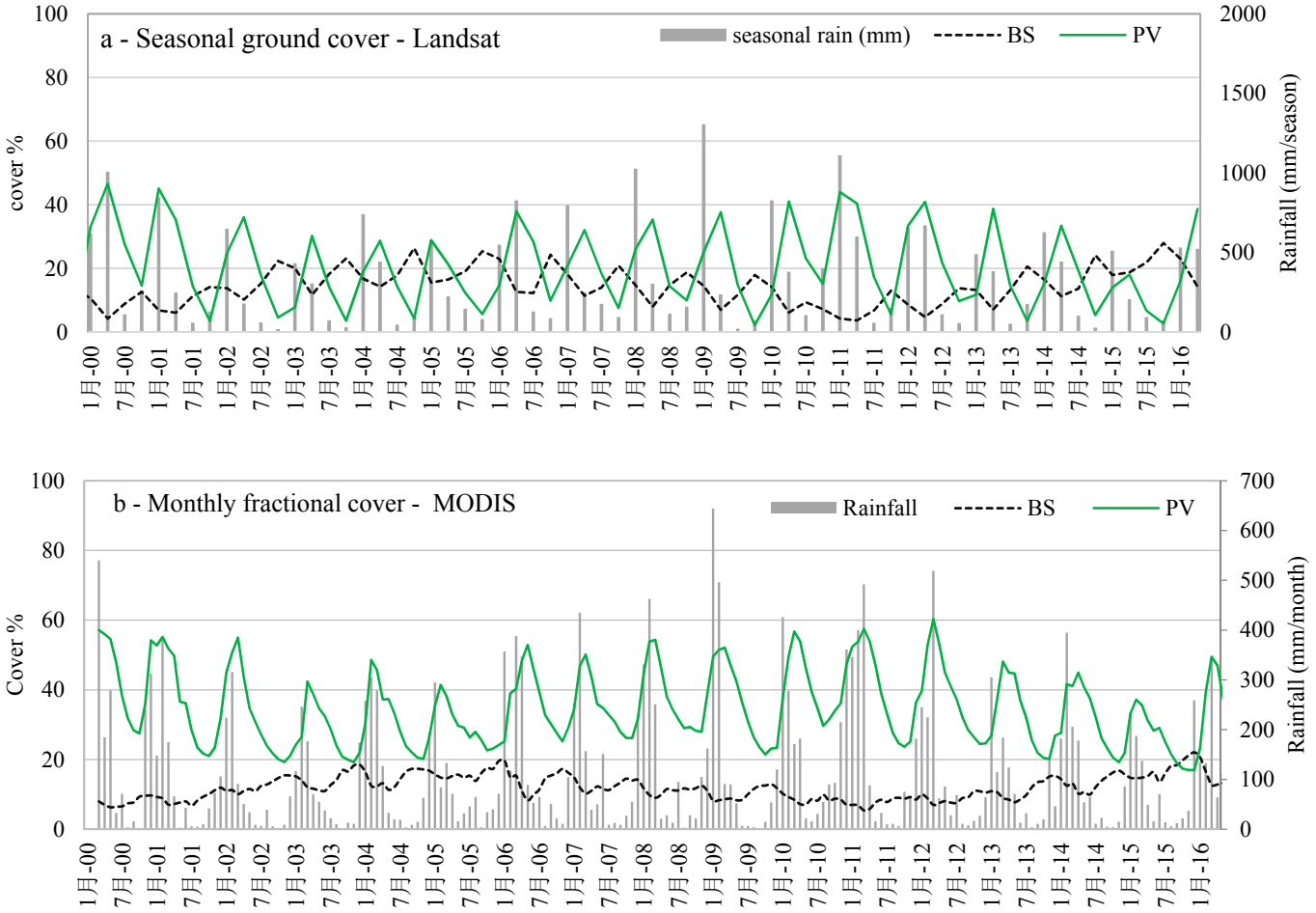

Figure 7. Seasonal and monthly ground cover changes in the Upper Burdekin. Part a – Seasonal Bare Soil (BS) of Photosynthetic Vegetation (PV) cover from Department of Science, Information Technology and Innovation remote sensing group ground cover data [53] from 2000-2016. Summer: December to February; Autumn: March to May; Winter: June to August; and Spring: September to November. Part b – monthly fractional cover extracted from MODIS datasets [45] from 2000-2016.

Annual soil water index (SWI) correlates positively with annual rainfall over the entire catchment (R^2 = 0.86). Although the monthly coefficient of determination of SWI and rainfall is lower (R^2 = 0.47) than annual, it follows a similar trend as rainfall. We used total rainfall in the prior year as a surrogate for antecedent soil moisture. The correlation analysis was performed between runoff ratio (RRt) and total rainfall of the prior year (P_{t-1}) and the prior two years (P_{t-2} + P_{t-1}). There is a high coefficient of determination between runoff ratio and antecedent precipitation for both cases. Interestingly, the R^2 between runoff ratio (RRt) and cumulative soil moisture of the two previous years (P_{t-2} + P_{t-1}) was even higher (R^2 = 0.80) than only using soil moisture for the previous year (R^2 = 0.77). This result indicates that the persistent woody cover is responding more to these 2-year deeper soil moisture stores compared to recurrent grass cover [64]. Annual RR correlates best with the maximum monthly runoff in the same year (R^2 = 0.87).

In the Upper Burdekin, on average, ground cover in November (25% end of dry season) is 25% lower than in April (50% end of wet season). Assuming ground cover influences large-scale runoff generation, we expected less runoff in April than November due to higher vegetation cover. However, results show the opposite effects with more runoff in April (10 mm) than November (3 mm) for similar size storms (>50 mm). This result can be explained by differences in antecedent soil moisture between November and April. Additional investigations of the relationship between runoff and other parameters revealed that catchment monthly runoff was highly correlated with rainfall (R vs. P: R^2 = 0.70) followed by antecedent soil moisture (runoff vs. soil moisture: R^2 = 0.30) and ground cover (runoff vs. ground cover: R^2 = 0.30). This agrees with plot scale findings that showed that rainfall intensity had a greater influence on runoff generation than ground cover [19]. At the beginning of the wet season, soil moisture and ground cover both influence (higher R^2 values, Table 3) runoff generation, but later (in March and April) the R^2's decrease as ground cover and soil moisture increase. This highlights the critical role of ground cover at the start of the wet season and how runoff generation is more sensitive to savanna ground cover in drier months than wetter months [19,21]. Very low R^2's between runoff and antecedent soil moisture in wetter months (Table 3) could be due to the saturation of riparian areas and other hydrologically active regions of the catchment [65].

Thus, at these assessment scales (annual, seasonal and relatively large catchments), we there was no significant effect of ground cover on runoff. In other words, fluctuations in mean annual ground cover (MODIS-derived total cover 81% - 91%) is not sufficient to detect changes in annual runoff. We conclude that for the full size range of catchments (193 – 36,260 km^2), runoff generation processes are sensitive to antecedent soil moisture conditions at all scales and ground cover at finer scales, but interactions between these two parameters may occur. This highlights the complex interaction between climate and land management in rangeland environments that complicates the interpretation of data on condition and trend of ground cover [25,66,67]. Therefore higher spatial resolution of ground cover data in shorter time periods (monthly and weekly) is needed to distinguish the effects of soil surface conditions on runoff generation processes.

Table 3. Coefficient of determination between monthly runoff and three parameters: rainfall, antecedent soil moisture and ground cover. Total rainfall of two previous months is used as an indicator of soil moisture. Gainsford and Valley of Lagoons are excluded due to shorter data records.

	Rainfall - runoff						**Soil moisture - runoff**						**Ground cover - runoff**					
	Nov	Dec	Jan	Feb	Mar	Apr	Nov	Dec	Jan	Feb	Mar	Apr	Nov	Dec	Jan	Feb	Mar	Apr
Upper Burdekin	0.56	0.85	0.68	0.65	0.77	0.54	0.45	0.61	0.30	0.52	0.01	0.22	0.49	0.58	0.41	0.23	0.34	0.33
Keelbottom	0.66	0.82	0.58	0.72	0.86	0.87	0.59	0.43	0.01	0.37	0.00	0.11	0.29	0.38	0.05	0.20	0.03	0.11
Basalt	0.71	0.82	0.67	0.55	0.65	0.24	0.75	0.42	0.21	0.28	0.01	0.08	0.69	0.50	0.28	0.15	0.29	0.25
Blue Range	0.58	0.83	0.64	0.63	0.68	0.73	0.51	0.73	0.31	0.49	0.00	0.06	0.47	0.63	0.29	0.12	0.14	0.18
Mount Fullstop	0.59	0.82	0.70	0.60	0.75	0.65	0.56	0.74	0.32	0.49	0.00	0.09	0.53	0.64	0.33	0.13	0.23	0.26
Laroona	0.60	0.84	0.68	0.79	0.92	0.80	0.34	0.36	0.04	0.49	0.01	0.12	0.40	0.31	0.15	0.28	0.22	0.25
Mount Bradley	0.58	0.86	0.79	0.71	0.93	0.69	0.32	0.44	0.04	0.55	0.03	0.08	0.43	0.30	0.21	0.33	0.14	0.11
Average	**0.61**	**0.84**	**0.68**	**0.66**	**0.79**	**0.64**	**0.50**	**0.53**	**0.18**	**0.46**	**0.01**	**0.11**	**0.47**	**0.48**	**0.24**	**0.21**	**0.20**	**0.21**

4.3. Changes in soil moisture conditions

Water balance analysis showed that the average of annual water balance from 1998 to 2014 is close to zero (+15 mm) indicating explicitly wet and dry periods in each individual year (i.e., water year starts in July with an empty bucket, then progressively fills, and then empties at the end of the water year in June). Water storage at the end of the water year (July-June) is positive for years with above average annual rainfall. For example, in most (i.e., 6 of 8) of the examined catchments, the water balance was positive in 2008-2009 and 2010-2011. This carryover water is stored as soil moisture in deeper soil profiles and trees extract water from deeper in the soil to maintain transpiration in dry years [26,68-70]. A small amount of this water in riparian corridors of major channels may feed baseflow.

Monthly water balance analysis showed that monthly runoff, actual evapotranspiration, and water storage follow the same trend as summer rainfall (Figure 8). All the water balance elements (i.e., rainfall, runoff, water storage, and evapotranspiration) are lowest in August to October and begin to increase in November at the start of the wet season. These parameters are higher from January through March than during the rest of the year. Water storage is positive from November through February (Figure 8 d), indicating that this is an energy-limited period (rainfall > runoff + evapotranspiration) and the soil "bucket" is filling with excess available water. This agrees with findings of a small-scale study in which wet season rainfall rapidly filled the soil and caused water to drain below the root-zone if the vegetation was unable to extract the water [54]. In contrast, the March to October period is water-limited with demands for evapotranspiration higher than available rain water. The water deficit in this period is supplied from water stored during the November through February wet period. Monthly runoff is at a maximum in February following the maximum monthly storage in January. Evapotranspiration is highest in March due to higher water availability in the previous two months (Figure 8c and 8d). There is a sharp decline in catchment water storage in March, most likely due to higher evapotranspiration because of greater vegetation cover near the end of the wet season (March) (Figure 8d). As evidence for this, monthly AET data follows the same trend as monthly green cover ($R^2 = 0.75$) and peak AET (Figure 8) coincides with green cover peaks (Figure 7) in the wet season.

These monthly water analyses indicate that runoff generation in January and February is influenced by saturation overland flow due to nearly saturated soil profiles in selected portions of the catchment. These areas are probably confined to riparian corridors, swales, and areas of shallow soil (Figure 9), which are most likely to become saturated. Soil bucket size is also an important factor in determining soil water holding capacity. Figure 9 represents soil depth of the Upper Burdekin catchment that can be used as rough macroscopic estimate of soil bucket size and potential parts of the catchment that would most likely have saturated components. By March and continuing through October, the soil bucket starts to empty by evapotranspiration and Hortonian overland flow becomes the dominant, if not exclusive, flow generation process. As also indicated by McIvor, Williams and Gardener [19], this infiltration-excess runoff is highly related to rainfall intensity in savanna rangelands.

The rainfall threshold analysis showed that for both monthly and annual time periods runoff at the catchment outlet is highly correlated with the number of storms during the wet season that exceeded 5 mm. Minor (< 5 mm) rainfall events are lower than total transmission losses (infiltration, evaporation and terminal water storage) of catchments and never reach catchment outlets [71]. This finding agrees with results of Roth [21] that showed relatively high infiltration rates at the beginning of events for this area using a rainfall simulator in small plots.

Therefore, in the Upper Burdekin with high rainfall intensities and low infiltration rates, Hortonian overland flow is the dominant runoff generation mechanism [21], with saturation overland flow becoming important in a few months that have higher opportunities for soil saturation [19]. In contrast, subsurface flow is more common in catchments with deep soils and soils with high hydraulic conductivities and infiltration rates; in these catchments very little surface runoff is generated during very high rainfall intensities [72,73].

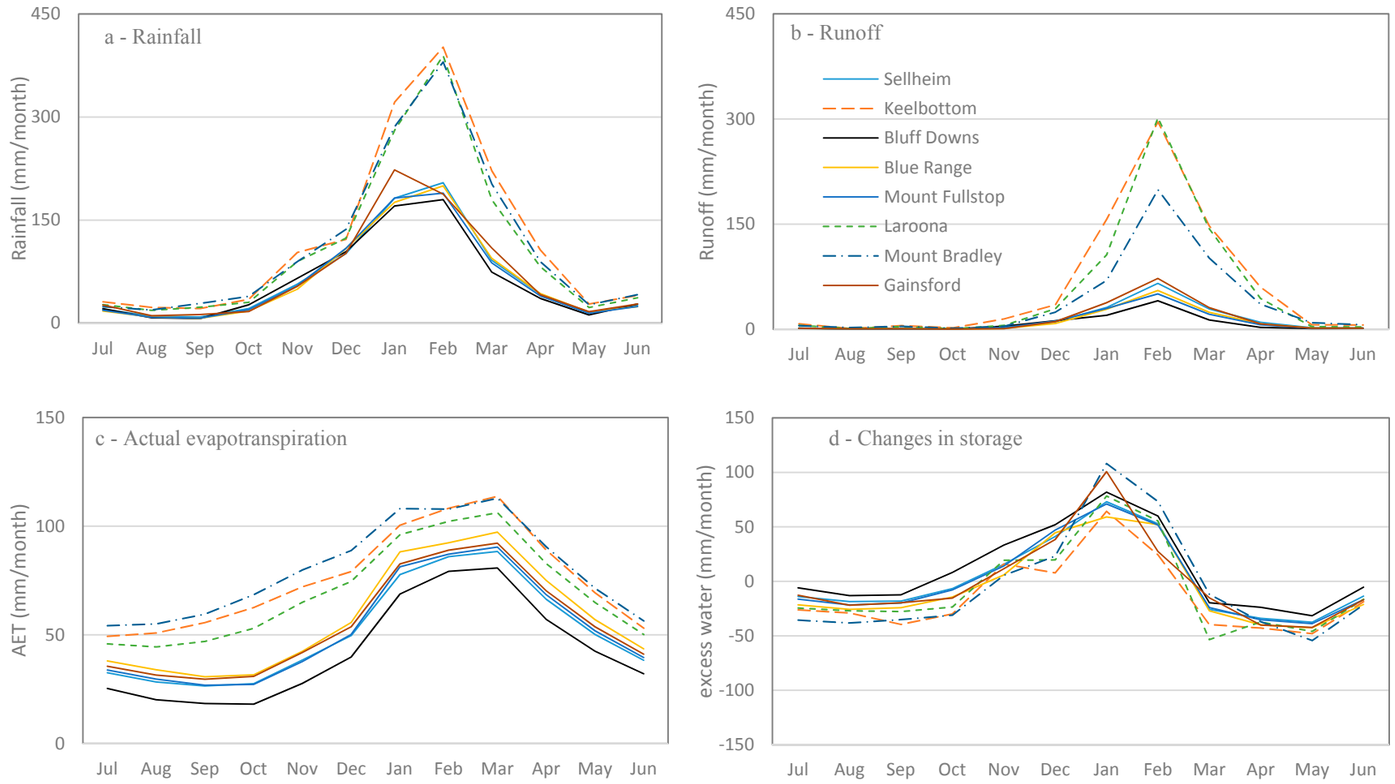

Figure 8. Monthly water balance calculations for catchments based on rainfall, runoff and evapotranspiration during 2000 to 2014, except for Gainsford that started in 2004. Water storage is calculated based on Eq. 1 by subtracting runoff and evapotranspiration from rainfall data for each month.

Preprints (www.preprints.org) | NOT PEER-REVIEWED | Posted: 13 June 2017 doi:10.20944/preprints201706.0056.v1

Peer-reviewed version available at Water 2017, 9, 540; doi:10.3390/w9070540

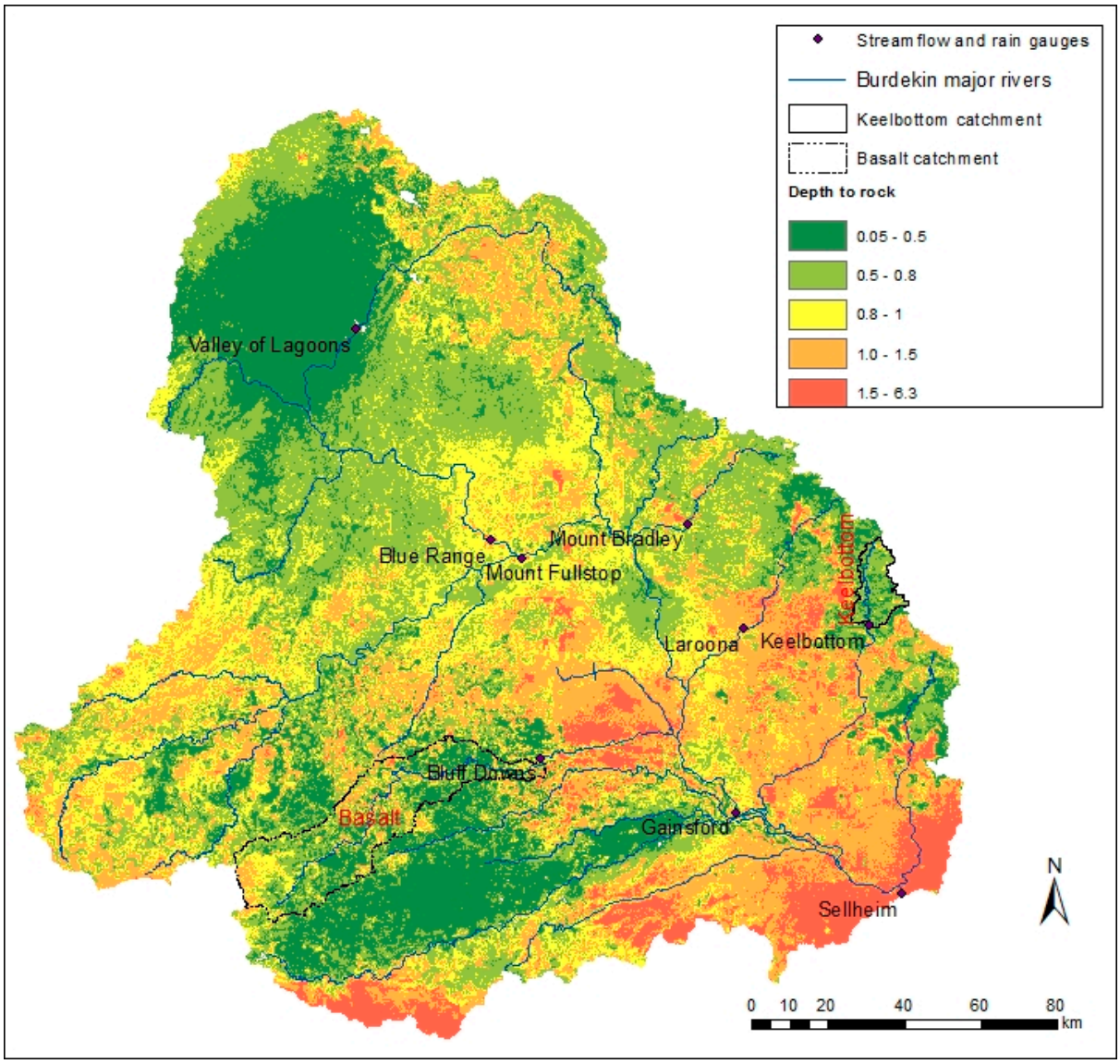

Figure 9. Depth to bedrock map of Upper Burdekin catchment. This map extracted from Queensland digital soil attributes-Burdekin River basin-depth to rock data (http://www.qld.gov.au/environment/land/soil/).

5. Conclusions

Spatial and temporal rainfall variability and rainfall-runoff relationships are examined in a large savannah catchment of Queensland, Australia. Hydroclimatic parameters are highly variable in space and time. During the distinct wet and dry seasons, specific hydrological processes dominate runoff generation. The wet season occurs from November to March with higher water availability from rainfall, and consequently higher runoff, soil moisture and actual evapotranspiration. The dry season from April through October has lower rainfall and runoff, and the stored water in the soil profile is gradually depleted via evapotranspiration due to the higher vegetation cover. The soil "bucket" empties towards the end of dry season in October. It is likely that both saturation overland and Hortonian overland flow contribute to runoff generation during the wet season due to higher water availability to soil profile, while during the dry season Hortonian overland flow (infiltration-

excess runoff) strongly dominates. Using moderate spatial resolution seasonal Landsat-derived ground cover products at a range of spatial (193 – 36,260 km²) and temporal (daily, monthly and annual) scales, it is difficult to distinguish between the effects of ground cover changes and climate variability on runoff generation process. Thus, we conclude that these effects are more clearly expressed, and changes potentially measurable, over smaller areas and time periods than the scales assessed in this paper. This type of coarse catchment-scale hydrological assessment improves our understanding of the dominant processes and drivers of runoff. We believe that such in-depth, catchment-based understanding is critical to bridge the gap between small-scale and large-scale studies, and to assist with upscaling results from data-rich plot scale studies to more applicable, broad catchment scales. Therefore, to separate ground cover and climate variability effects, we should focus on in-depth rainfall-runoff processes by using finer resolution datasets in a process-based hydrological model of smaller (< 100 km²) catchments. The results of this study can be used to better understand the hydrological processes of dryland environments elsewhere in the world with similar rangeland and climate conditions and are critical to better understand the hydrological processes of dryland environments and subsequent effects of exposure of coral reef ecosystems in Australia to terrestrial runoff.

Acknowledgments: We thank Copernicus Global Land Service for providing Soil Water Index data. MOD16b Evapotranspiration data were provided by Numerical Terradynamic Simulation Group of The University of Montana. Seasonal and monthly ground cover were downloaded from Terrestrial Ecosystem Research Network, AusCover. Authors thank Queensland Government departments for providing rainfall and discharge data. Authors also would like to thank three CSIRO reviewers Dr John Gallant, Dr Tim McVicar and Dr Ralph Trancoso for their helpful comments, as well as _ anonymous reviewers and the Associate Editor. The authors would also like to acknowledge funding from the CSIRO and the National Environmental Science Program (NESP) Tropical Water Quality Hub.

Author Contributions: Ben Jarihani, Roy Sidle, Rebecca Bartley, Christian Roth and Scott Wilkinson designed the experiments; Ben Jarihani analyzed the data and wrote the paper; Roy Sidle, Rebecca Bartley, Christian Roth and Scott Wilkinson reviewed the paper.

Conflicts of Interest: The authors declare no conflict of interest.

References

1. De'ath, G.; Fabricius, K.E.; Sweatman, H.; Puotinen, M. The 27–year decline of coral cover on the great barrier reef and its causes. *Proceedings of the National Academy of Sciences* **2012**, *109* 17995-17999.
2. Edinger, E.N.; Jompa, J.; Limmon, G.V.; Widjatmoko, W.; Risk, M.J. Reef degradation and coral biodiversity in indonesia: Effects of land-based pollution, destructive fishing practices and changes over time. *Marine Pollution Bulletin* **1998**, *36*, 617-630.
3. Fabricius, K.; Logan, M.; Weeks, S.; Lewis, S.; Brodie, J. Changes in water clarity in response to river discharges on the great barrier reef continental shelf: 2002–2013. *Estuarine, Coastal and Shelf Science* **2016**, *173*, A1-A15.
4. Richmond, R.H. Coral reefs: Present problems and future concerns resulting from anthropogenic disturbance. *American Zoologist* **1993**, *33*, 524-536.
5. Rogers, C.S. Responses of coral reefs and reef organisms to sedimentation. *Marine ecology progress series. Oldendorf* **1990**, *62*, 185-202.

6. Sharples, J.; Middelburg, J.J.; Fennel, K.; Jickells, T.D. What proportion of riverine nutrients reaches the open ocean? *Global Biogeochemical Cycles* **2017**, *31*, 39-58.
7. Devlin, M.J.; Harkness, P.; McKinna, L.; Abbott, B.N.; Brodie, J. Exposure of riverine plume waters in the great barrier reef: Mapping of exposure and risk to gbr ecosystems. *Marine Pollution Bulletin* **2012**, *65*, 224-235.
8. Brodie, J.; Binney, J.; Fabricius, K.; Gordon, I.; Hoegh-Guldberg, O.; Hunter, H.M.; O'Reagain, P.; Pearson, R.; Quirk, M.; Thorburn, P.J.*, et al. Synthesis of evidence to support the scientific consensus statement on water quality in the great barrier reef*; Reef Water quality Protection Plan Secretariat: Brisbane, 2008.
9. Fabricius, K.E. Effects of terrestrial runoff on the ecology of corals and coral reefs: Review and synthesis. *Marine Pollution Bulletin* **2005**, *50*, 125-146.
10. Brodie, J.E.; Kroon, F.J.; Schaffelke, B.; Wolanski, E.C.; Lewis, S.E.; Devlin, M.; Bainbridge, Z.T.; Waterhouse, J.; Davis, A.M. Terrestrial pollutant runoff to the great barrier reef: An update of issues, priorities and management responses. *Marine Pollution Bulletin* **2012**, *65*.
11. Larsen, M.C.; Webb, R.M. Potential effects of runoff, fluvial sediment, and nutrient discharges on the coral reefs of puerto rico. *J. Coast. Res.* **2009**, 189-208.
12. Access, E.D. Economic contribution of the great barrier reef. **2013**.
13. Wenger, A.S.; Johansen, J.L.; Jones, G.P. Increasing suspended sediment reduces foraging, growth and condition of a planktivorous damselfish. *J. Exp. Mar. Biol. Ecol.* **2012**, *428*, 43-48.
14. McCloskey, G.; Waters, D.; Baheerathan, R.; Darr, S.; Dougall, C.; Ellis, R.; Fentie, B.; Hateley, L. *Modelling reductions of pollutant loads due to improved management practices in the great barrier reef catchments: Updated methodology and results - technical report for reef report card 2015*; Queensland Department of Natural Resources and Mines,, Brisbane, Queensland: 2017.
15. Furnas, M. Catchments and corals, terrestrial runoff to the great barrier reef 2003. *Australian Institute of Marine Science: Townsville, Qld* **2002**.
16. Thorburn, P.J.; Wilkinson, S.N.; Silburn, D.M. Water quality in agricultural lands draining to the great barrier reef: Causes, management and priorities *Agric. Ecosyst. Environ.* **2013**, *180*, 4-20.
17. Bartley, R.; Roth, C.H.; Ludwig, J.; McJannet, D.; Liedloff, A.; Corfield, J.; Hawdon, A.; Abbott, B. Runoff and erosion from australia's tropical semi-arid rangelands: Influence of ground cover for differing space and time scales. *Hydrological Processes* **2006**, *20*, 3317-3333.
18. Scanlan, J.C.; Pressland, A.J.; Myles, D.J. Run-off and soil movement on mid-slopes in north-east queensland grazed woodlands. *Rangelands Journal* **1996**, *18*, 33-46.
19. McIvor, J.G.; Williams, J.; Gardener, C.J. Pasture management influences runoff and soil movement in the semi-arid tropics. *Aust. J. Exp. Agric.* **1995**, *35*, 55-65.
20. Silburn, D.M.; Carroll, C.; Ciesiolka, C.A.A.; deVoil, R.C.; Burger, P. Hillslope runoff and erosion on duplex soils in grazing lands in semi-arid central queensland. I. Influences of cover, slope, and soil. *Soil Research* **2011**, *49*, 105-117.

21. Roth, C. A framework relating soil surface condition to infiltration and sediment and nutrient mobilisation in grazed rangelands of north-eastern queensland. *Earth Surface Processes and Landforms* **2004**, *29*, 1093-1104.
22. Ludwig, J.A.; Bartley, R.; Hawdon, A.; Abbott, B.; McJannet, D. Patch configuration non-linearly affects sediment loss across scales in a grazed catchment in north-east australia. *Ecosystems* **2007**, *10*, 839-845.
23. Post, D.A. Regionalizing rainfall-runoff model parameters to predict the daily streamflow of ungauged catchments in the dry tropics. *Hydrol. Res.* **2009**, *40*, 433-444.
24. Lough, J.M. Great barrier reef coral luminescence reveals rainfall variability over northeastern australia since the 17th century. *Paleoceanography* **2011**, *26*, 1-14.
25. Peña-Arancibia, J.L.; van Dijk, A.I.J.M.; Guerschman, J.P.; Mulligan, M.; Bruijnzeel, L.A.; McVicar, T.R. Detecting changes in streamflow after partial woodland clearing in two large catchments in the seasonal tropics. *Journal of Hydrology* **2012**, *416-417*, 60-71.
26. Leuning, R.; Cleugh, H.A.; Zegelin, S.J.; Hughes, D. Carbon and water fluxes over a temperate eucalyptus forest and a tropical wet/dry savanna in australia: Measurements and comparison with modis remote sensing estimates. *Agric. For. Meteorol.* **2005**, *129*, 151-173.
27. Thornton, C.M.; Cowie, B.A.; Freebairn, D.M.; Playford, C.L. The brigalow catchment study: Ii. Clearing brigalow (acacia harpophylla) for cropping or pasture increases runoff. *Australian Journal of Soil Research* **2007**, *45*, 496-511.
28. Siriwardena, L.; Finlayson, B.L.; McMahon, T.A. The impact of land use change on catchment hydrology in large catchments: The comet river, central queensland, australia. *Journal of Hydrology* **2006**, *326*, 199-214.
29. Bartley, R.; Corfield, J.P.; Hawdon, A.A.; Kinsey-Henderson, A.E.; Abbott, B.N.; Wilkinson, S.N.; Keen, R.J. Can changes to pasture management reduce runoff and sediment loss to the great barrier reef? The results of a 10-year study in the burdekin catchment, australia. *The Rangeland Journal* **2014**, *36*, 67-84.
30. Wohl, E.; Barros, A.; Brunsell, N.; Chappell, N.A.; Coe, M.; Giambelluca, T.; Goldsmith, S.; Harmon, R.; Hendrickx, J.M.H.; Juvik, J.*, et al.* The hydrology of the humid tropics. *Nature Clim. Change* **2012**, *2*, 655-662.
31. Trancoso, R.; Larsen, J.R.; McAlpine, C.; McVicar, T.R.; Phinn, S. Linking the budyko framework and the dunne diagram. *Journal of Hydrology* **2016**, *535*, 581-597.
32. Horton, R.E. The role of infiltration in the hydrologic cycle. *Eos, Transactions American Geophysical Union* **1933**, *14*, 446-460.
33. Dunne, T.; Black, R.D. Partial area contributions to storm runoff in a small new england watershed. *Water Resources Research* **1970**, *6*, 1296-1311.
34. Bartley, R.; Croke, J.; Bainbridge, Z.T.; Austin, J.M.; Kuhnert, P.M. Combining contemporary and long-term erosion rates to target erosion hot-spots in the great barrier reef, australia. *Anthropocene* **2015**, *10*, 1-12.
35. Bainbridge, Z.T.; Lewis, S.E.; Smithers, S.G.; Kuhnert, P.M.; Henderson, B.L.; Brodie, J.E. Fine - suspended sediment and water budgets for a large, seasonally dry tropical catchment: Burdekin river catchment, queensland, australia. *Water Resources Research* **2014**, *50*, 9067-9087.

36. Flood, N.; Danaher, T.; Gill, T.; Gillingham, S. An operational scheme for deriving standardised surface reflectance from landsat tm/etm+ and spot hrg imagery for eastern australia. *Remote Sensing* **2013**, *5*, 83.
37. Rossel, R.V.; Chen, C.; Grundy, M.; Searle, R.; Clifford, D.; Campbell, P. The australian three-dimensional soil grid: Australia's contribution to the globalsoilmap project. *Soil Research* **2015**, *53*, 845-864.
38. Rogers, L.; Cannon, M.; Barry, E. *Land resources of the dalrymple shire*; Department of Natural Resources and CSIRO: Brisbane, 1999.
39. Bartley, R.; Hawdon, A.; Post, D.A.; Roth, C.H. A sediment budget in a grazed semi-arid catchment in the burdekin basin, australia. *Geomorphology* **2007**, *87*, 302-321.
40. Isbell, R. *The australian soil classification*. CSIRO publishing: 2016.
41. Raupach, M.; Briggs, P.; Haverd, V.; King, E.; Paget, M.; Trudinger, C. Australian water availability project (awap). *CSIRO Marine and Atmospheric Research Component: final report for phase* **2008**, *2*, 38.
42. Jeffrey, S.J.; Carter, J.O.; Moodie, K.B.; Beswick, A.R. Using spatial interpolation to construct a comprehensive archive of australian climate data. *Environmental Modelling & Software* **2001**, *16*, 309-330.
43. Jones, D.A.; Wang, W.; Fawcett, R. High-quality spatial climate data-sets for australia. *Australian Meteorological and Oceanographic Journal* **2009**, *58*, 233.
44. Mu, Q.; Zhao, M.; Running, S.W. Improvements to a modis global terrestrial evapotranspiration algorithm. *Remote Sensing of Environment* **2011**, *115*, 1781-1800.
45. Guerschman, J.P.; Scarth, P.F.; McVicar, T.R.; Renzullo, L.J.; Malthus, T.J.; Stewart, J.B.; Rickards, J.E.; Trevithick, R. Assessing the effects of site heterogeneity and soil properties when unmixing photosynthetic vegetation, non-photosynthetic vegetation and bare soil fractions from landsat and modis data. *Remote Sensing of Environment* **2015**, *161*, 12-26.
46. Copernicus Service information. Soil water index. http://land.copernicus.eu/global/products/swi
47. Wagner, W. *Soil moisture retrieval from ers scatterometer data*. Citeseer: 1998.
48. Albergel, C.; Rüdiger, C.; Pellarin, T.; Calvet, J.-C.; Fritz, N.; Froissard, F.; Suquia, D.; Petitpa, A.; Piguet, B.; Martin, E. From near-surface to root-zone soil moisture using an exponential filter: An assessment of the method based on in-situ observations and model simulations. *Hydrology and Earth System Sciences Discussions* **2008**, *12*, 1323-1337.
49. FAO, C. A computer program for irrigation planning and management. *Irrigation and Drainage Paper* **2009**, *46*.
50. Faurès, J.-M.; Goodrich, D.C.; Woolhiser, D.A.; Sorooshian, S. Impact of small-scale spatial rainfall variability on runoff modeling. *Journal of Hydrology* **1995**, *173*, 309-326.
51. (USDA), U.S.D.o.A. Rist - rainfall intensity summarization tool. http://www.ars.usda.gov/Research/docs.htm?docid=3251 (11th August),
52. McGregor, K.; Bingner, R.; Bowie, A.; Foster, G. Erosivity index values for northern mississippi. *Transactions of the ASAE* **1995**, *38*, 1039-1047.
53. Trevithick, R.; Scarth, P.; Tindall, D.; Denham, R.; Flood, N. *Cover under trees: Rp64g synthesis report*; Department of Science, Information Technology, Innovation and the Arts: Brisbane, 2014.

54. Williams, J.; Bui, E.N.; Gardner, E.A.; Littleboy, M.; Probert, M.E. Tree clearing and dryland salinity hazard in the upper burdekin catchment of north queensland. *Australian Journal of Soil Research* **1997**, *35*, 785-801.
55. Budyko, M. Climate and life, 508 pp. Academic Press, New York: 1974.
56. McVicar, T.R.; Roderick, M.L.; Donohue, R.J.; Van Niel, T.G. Less bluster ahead? Ecohydrological implications of global trends of terrestrial near-surface wind speeds. *Ecohydrology* **2012**, *5*, 381-388.
57. Petheram, C.; McMahon, T.A.; Peel, M.C. Flow characteristics of rivers in northern australia: Implications for development. *Journal of Hydrology* **2008**, *357*, 93-111.
58. Trancoso, R.; Phinn, S.; McVicar, T.R.; Larsen, J.R.; McAlpine, C.A. Regional variation in streamflow drivers across a continental climatic gradient. *Ecohydrology* **2016**, n/a-n/a.
59. Trancoso, R.; Phinn, S.; McVicar, T.R.; Larsen, J.R.; McAlpine, C.A. Regional variation in streamflow drivers across a continental climatic gradient. *Ecohydrology* **2017**, e1816-n/a.
60. Yang, Y.; Donohue, R.J.; McVicar, T.R. Global estimation of effective plant rooting depth: Implications for hydrological modeling. *Water Resources Research* **2016**, *52*, 8260-8276.
61. Sidle, R.C.; Tsuboyama, Y.; Noguchi, S.; Hosoda, I.; Fujieda, M.; Shimizu, T. Seasonal hydrologic response at various spatial scales in a small forested catchment, hitachi ohta, japan. *Journal of Hydrology* **1995**, *168*, 227-250.
62. Tsuboyama, Y.; Sidle, R.C.; Noguchi, S.; Murakami, S.; Shimizu, T. A zero-order basin—its contribution to catchment hydrology and internal hydrological processes. *Hydrological Processes* **2000**, *14*, 387-401.
63. Wilkinson, S.N.; Dougall, C.; Kinsey-Henderson, A.E.; Searle, R.; Ellis, R.; Bartley, R. Development of a time-stepping sediment budget model for assessing land use impacts in large river basins. *Science of the Total Environment* **2014**, *468-469*, 1210-1224.
64. Donohue, R.J.; McVicar, T.R.; Roderick, M.L. Climate-related trends in australian vegetation cover as inferred from satellite observations, 1981–2006. *Glob. Change Biol.* **2009**, *15*, 1025-1039.
65. McDonnell, J.J. Where does water go when it rains? Moving beyond the variable source area concept of rainfall‐runoff response. *Hydrological processes* **2003**, *17*, 1869-1875.
66. Bastin, G.; Scarth, P.; Chewings, V.; Sparrow, A.; Denham, R.; Schmidt, M.; O'Reagain, P.; Shepherd, R.; Abbott, B. Separating grazing and rainfall effects at regional scale using remote sensing imagery: A dynamic reference-cover method. *Remote Sensing of Environment* **2012**, *121*, 443-457.
67. Scarth, P.; Röder, A.; Schmidt, M.; Denham, R. In *Tracking grazing pressure and climate interaction—the role of landsat fractional cover in time series analysis*, Proceedings of the 15th Australasian Remote Sensing and Photogrammetry Conference, Alice Springs, Australia, 2010; pp 13-17.
68. Beringer, J.; Hutley, L.B.; Hacker, J.M.; Neininger, B.; Paw U, K.T. Patterns and processes of carbon, water and energy cycles across northern australian landscapes: From point to region. *Agric. For. Meteorol.* **2011**, *151*, 1409-1416.
69. Cernusak, L.A.; Hutley, L.B.; Beringer, J.; Holtum, J.A.M.; Turner, B.L. Photosynthetic physiology of eucalypts along a sub-continental rainfall gradient in northern australia. *Agric. For. Meteorol.* **2011**, *151*, 1462-1470.

70. Hutley, L.B.; Beringer, J.; Isaac, P.R.; Hacker, J.M.; Cernusak, L.A. A sub-continental scale living laboratory: Spatial patterns of savanna vegetation over a rainfall gradient in northern australia. *Agric. For. Meteorol.* **2011**, *151*, 1417-1428.

71. Jarihani, A.A.; Larsen, J.R.; Callow, J.N.; McVicar, T.R.; Johansen, K. Where does all the water go? Partitioning water transmission losses in a data-sparse, multi-channel and low-gradient dryland river system using modelling and remote sensing. *Journal of Hydrology* **2015**, *529, Part 3*, 1511-1529.

72. Lane, P.N.J.; Croke, J.C.; Dignan, P. Runoff generation from logged and burnt convergent hillslopes: Rainfall simulation and modelling. *Hydrological Processes* **2004**, *18*, 879-892.

73. Sarkar, R.; Dutta, S.; Dubey, A.K. An insight into the runoff generation processes in wet sub-tropics: Field evidences from a vegetated hillslope plot. *CATENA* **2015**, *128*, 31-43.